THE ASTROPHYSICAL JOURNAL, 546:165–175, 2001 January 1

ON THE EFFECT OF CHAOTIC ORBITS ON DYNAMICAL FRICTION

SOFÍA A. CORA, M. MARCELA VERGNE, AND JUAN C. MUZZIO
Facultad de Ciencias Astronómicas y Geofísicas, Universidad Nacional de La Plata; and Instituto de Astrofísica de La Plata del Consejo Nacional de Investigaciones Científicas y Técnicas de la República Argentina, Observatorio Astronómico, Paseo del Bosque s/n, 1900 La Plata, Argentina
Received 1999 October 15; accepted 2000 August 11

ABSTRACT

Chaotic orbits suffer significant changes as a result of small perturbations. One can thus wonder whether the dynamical friction suffered by a satellite on a regular orbit, and interacting with the stars of a galaxy, will be different if the bulk of the stars of the galaxy are in regular or chaotic orbits. In order to check that idea, we investigated the orbital decay (caused by dynamical friction) of a rigid satellite moving within a larger stellar system (a galaxy) whose potential is nonintegrable. We performed numerical experiments using two kinds of triaxial galaxy models: (1) the triaxial generalization of Dehnen's spherical mass model (Dehnen; Merritt & Fridman); (2) a modified Satoh model (Satoh; Carpintero, Muzzio, & Wachlin). The percentages of chaotic orbits present in these models were increased by perturbing them. In the first case, a central compact object (black hole) was introduced; in the second case, the perturbation was produced by allowing the galaxy to move on a circular orbit in a logarithmic potential. The equations of motion were integrated with a non–self-consistent code. Our results show that the presence of chaotic orbits does not affect significantly the orbital decay of the satellite.

Subject headings: galaxies: interactions — galaxies: kinematics and dynamics — methods: numerical

1. INTRODUCTION

Chaotic orbits can appear in stellar systems for several reasons, such as density gradients in the core, flattening, and rotation. In the case of elliptical galaxies, with an almost nonrotating figure and where the dynamics is free of gas, the presence of chaotic orbits is attributed to the galaxy's triaxial shape and to the central perturbations (e.g., Udry & Pfenniger 1988; Merritt & Fridman 1996). The inclusion of central singularities, containing a large fraction of galaxy mass, has a substantial influence on the dynamics and evolution of the surrounding stars, mainly affecting the box orbits present in triaxial systems (Gerhard & Binney 1985). These models are supported by *Hubble Space Telescope* observations (Crane et al. 1993; Jaffe et al. 1994; Ferrarese et al. 1994; Lauer et al. 1995) that show that elliptical galaxies and bulges of spiral galaxies exhibit a variety of cusp strengths and possible central black holes (Ford et al. 1994; Miyoshi et al. 1995). For the spiral barred galaxies, the chaotic trajectories may be important owing to the rotation of the figure and the bar perturbation (Contopoulos & Papayannopoulos 1980; Contopoulos 1983; Athanassoula et al. 1983; Pfenniger 1984) and to the effects of the gas that joins the bar and the spiral arms (Contopoulos & Grosbol 1989). Finally, Carpintero, Muzzio, & Wachlin (1999, hereafter CMW), Muzzio, Carpintero, & Wachlin (2000a), and Muzzio, Wachlin, & Carpintero (2000b) have recently shown that, inside the stellar system they analyzed, chaotic stellar orbits are very common, and, in some cases, they may outnumber the regular orbits.

Given the presence of chaotic orbits in some stellar systems, one can wonder whether the dynamical friction (Chandrasekhar 1943) suffered by a body moving within such systems differs from the one it would be subject to in the presence of regular orbits only. There is no study on this subject aside from the interesting, but limited, one by Pfenniger (1986). Pfenniger discussed the different responses of regular and chaotic orbits to perturbations and concluded that relaxation times in nonintegrable potentials might be orders of magnitude lower than in integrable potentials. He referred only briefly and tangentially to dynamical friction, mainly through its relationship to the relaxation time (his eq. [2]), but he indicated that although irregular orbits suffer a larger friction, this does not mean that dynamical friction on the whole system is necessarily stronger. Now, it is clear that a chaotic orbit may suffer large changes as a result of interstellar encounters, but it is doubtful whether that effect can be called dynamical friction in the sense used by Chandrasekhar. As the change in the orbit is mainly due to the properties of the orbit itself, one cannot indicate a priori what will happen to the orbit; for example, there is no guarantee that a satellite on a chaotic orbit will tend to fall toward the center of the system, as a satellite on a regular orbit would do, because the orbital changes due to chaoticity will probably, as indicated by Pfenniger, be more important than the general slowing down envisaged by Chandrasekhar. We are interested, instead, in the dynamical friction experienced by a body moving on a regular orbit within a stellar system with a large fraction of stars on chaotic orbits. Let us follow Chandrasekhar's view and regard dynamical friction as being due to the accumulation of the effects of successive encounters between the body and individual stars. We may reason that, if stellar motions are more significantly altered when the corresponding orbits are chaotic, then, by reaction, the motion of the body will be more affected than when the stellar motions are only slightly perturbed because they are on regular orbits. One might thus expect dynamical friction to increase in the presence of chaotic orbits.

A popular way to investigate dynamical friction is through the orbital decay of a galactic satellite. Nevertheless, it should be recalled that orbital decay is a very complex phenomenon in which several physical processes intervene (dynamical friction, tidal deformations of both the galaxy and the satellite, mass loss due to the interaction, etc.). As a result, there are widely different opinions among different authors (Bontekoe & van Albada 1987; Zaritsky &

White 1988; Weinberg 1989; Tremaine & Weinberg 1984; Séguin & Dupraz 1994, 1996), most of them summarized by Cora, Muzzio, & Vergne (1997, hereafter CMV), who performed their own numerical experiments on orbital decay of galactic satellites and added some conclusions of their own. In order to evaluate dynamical friction from the orbital decay of a satellite, the numerical experiments must be designed so as to avoid that other effects influence the results. From the start, it is obvious that one must use a single-body, undeformable, satellite to prevent mass loss and structural changes from affecting the results (Prugniel & Combes 1992; Colpi, Mayer, & Gobernato 1999). Structural changes in the galaxy are more difficult to avoid, as the orbital decay of the satellite necessarily injects energy in the galaxy, but CMV showed that for low-mass satellites (typically, 1/100 the mass of the galaxy or less), the changes in the galaxy are small enough to not alter the results.

Another very useful finding of CMV was that essentially the same orbital decay results are obtained with self-consistent and non–self-consistent codes. This result was not obtained by Hernquist & Weinberg (1989) because of their definition of non–self-consistency, in which the potential field is fixed in time and is not allowed to move spatially. This is the numerical analog of the non–self-consistent analysis performed by Weinberg (1989). To avoid confusion because of the use of the term *self-consistency*, let us emphasize here that, for us, a self-consistent code is one in which the potential is derived from the distribution of particles itself, while in a non–self-consistent code, the form of the potential is fixed in time (it does not change as the particle distribution does), although it is allowed to move spatially around the center of mass of the galaxy-satellite system. This result of CMV is very useful for our present work because, on the one hand, non–self-consistent codes are simpler and run much faster in a computer, and, on the other hand, one does not need to generate initial conditions that correspond to a self-consistent system. Nevertheless, it is worth recalling that some caution is needed to avoid undesirable effects. For example, it is well known after White (1983) that both the galaxy and the satellite should be allowed to rotate around their common center of gravity, as the seemingly innocent idea of fixing the center of the galaxy and letting the satellite rotate around it spuriously and dramatically changes the orbital decay times (in fact, Weinberg's different definition of self-consistency is related to this effect). It is worth noting that, with our non–self-consistent method, the distribution of particles reacts to the presence of the satellite, thus ensuring that effects such as the formation of a wake are included in the simulation. Only second-order effects, such as the action of the field of the wake on its own distribution, are ignored, but these are negligibly small for satellites of low mass, as indicated. Our method is similar to the multiple three-body algorithm (MTBA) of Borne (1984), used by Séguin & Dupraz (1994), who also concluded that self-gravity is a minor ingredient of the global process. The moderate effect of self-gravity on dynamical friction was also noted by Wahde, Donner, & Sundelius (1996), who also found that the effect of velocity dispersion is small; it is worth recalling, however, that their work refers to disk galaxies only.

Thus, we decided to investigate the sensitivity of dynamical friction to the presence of chaotic orbits by means of non–self-consistent numerical simulations of the orbital decay of a satellite inside a galaxy. The basic idea was to use pairs of galaxy models such that both members of the pair have similar density and velocity distributions, but with one of them (called the "basic model") made up of stars mainly on regular orbits, and the other one (called the "chaotic model") including a large fraction of chaotic orbits. Although the idea is simple in principle, it turned out to be very difficult to find pairs of models with those properties. Nevertheless, as we are interested in checking the importance of a particular physical effect, there is no need to use models that mimic real galaxies, but purely theoretical models are perfectly suitable as well. In fact, one of the advantages of numerical experiments is that we can add or suppress at will certain effects in order to isolate better the process we want to study. Taking into account that the chaotic regions of the phase space of a nonintegrable potential grow when a perturbation is introduced, we can take as one member of those pairs a model with a slightly nonintegrable potential (which has few chaotic orbits) and, as the other member, the same model with a perturbation added (to increase the number of chaotic orbits).

The central cusp models used by Merritt & Fridman (1996) are adequate candidates for the present purpose, particularly considering that our use of non–self-consistent methods prevents any evolution of the system toward axisymmetry (Merritt & Fridman 1996; Valluri & Merritt 1998; Merritt & Quinlan 1998) with the possible decrease of the percentage of chaotic orbits. Another way of perturbing the system is by means of rotation, which may yield a high degree of chaoticity (CMW; Muzzio et al. 2000a, 2000b). These two different types of perturbations affect different orbit families in the models: the central compact object perturbs box orbits more effectively, while the rotation used by CMW affects more strongly the tube orbits. Of course, the effect of the perturbation should be included in the equations of motion of the particles that make up the galaxy, but not in those of the satellite. In that way, were it not for the particle-satellite interactions, the orbit of the satellite would be the same in the models with and without perturbation; any departures can then be attributed to the different sort of stellar orbits (regular or chaotic) present in each model.

Section 2 gives the details of the numerical code used to perform the simulations, as well as the numerical techniques employed to carry out the orbital classification in each model. The properties of the triaxial models considered, and of the perturbations introduced in each case, are described in §§ 3 and 4, respectively. The results of the orbital classification performed in each case to determine the percentage of chaotic orbits present in the models used are also given in these sections, together with the results of the simulations. Finally, § 5 discusses the results obtained in §§ 3 and 4.

2. NUMERICAL TECHNIQUES

2.1. *Integration Code*

We have shown before (CMV) that it is irrelevant for dynamical friction investigations whether the interactions among the particles that make up the galaxy are taken into account or not. Therefore, we adopted a non–self-consistent code in which the galaxy and the satellite are represented with rigid potentials; the particles that make up the galaxy interact with these two rigid potentials, but not among themselves, while the motion of the satellite is governed exclusively by its interactions with those particles. Thus, the

equations of motion are

$$\frac{d^2\boldsymbol{r}_i}{dt^2} = -\nabla\Phi(\boldsymbol{r}_i) - \frac{Gm_s(\boldsymbol{r}_i - \boldsymbol{r}_s)}{(\varepsilon_s^2 + |\boldsymbol{r}_i - \boldsymbol{r}_s|^2)^{3/2}},$$

$$\frac{d^2\boldsymbol{r}_s}{dt^2} = -\sum_{i=1}^{N} \frac{Gm_i(\boldsymbol{r}_s - \boldsymbol{r}_i)}{(\varepsilon_s^2 + |\boldsymbol{r}_s - \boldsymbol{r}_i|^2)^{3/2}}. \quad (1)$$

The first equation is valid for the N particles that make up the galaxy ($i = 1, \ldots, N$), each one of mass m_i ($\equiv M/N$, M being the total mass of the galaxy), and Φ is the potential that represents the galaxy. The second equation corresponds to the satellite, of mass m_s and softening parameter ε_s, and G is the gravitational constant. The vectors $\boldsymbol{r}_i$ and $\boldsymbol{r}_s$ give the positions of the particles and of the satellite, respectively, which are referred to the center of mass of the galaxy-satellite system. The equations of motions were integrated using a seventh-/eighth-order Runge-Kutta-Fehlberg routine.

Our equations of motion do not guarantee that the sum of all the internal forces on the particles at positions $\boldsymbol{r}_i$, $\nabla\Phi(\boldsymbol{r}_i)$, equals zero. Since this may cause a nonphysical acceleration of the galaxy, small corrections to the accelerations were introduced at each integration step for all particles. These corrections coincide with the mean internal acceleration of the galaxy ($[\sum_{i=1}^{N} \nabla_x \Phi(\boldsymbol{r}_i)]/N$, for the x coordinate; similar expressions are valid for the other ones). In this way, the sum of the internal forces is cancelled.

This procedure yielded a good conservation of the total linear momentum and energy of the galaxy-satellite system; the fractional energy variations were kept below $|\Delta E|/|E| \sim 5 \times 10^{-6}$ for time intervals of 20 crossing times.

2.2. *Orbital Classification*

After choosing the "basic model" (to represent the galaxy) and the perturbation (that was introduced to obtain the "chaotic model") we had to classify the orbits in each model in order to determine whether they behaved regularly or chaotically and to make sure that the latter model had a substantially larger number of chaotic orbits than the former.

A standard way of detecting and quantifying chaoticity is through the computation of the Liapunov characteristic exponents (e.g., Lichtenberg & Lieberman 1992), which give the mean exponential rates of divergence from a given trajectory. They are defined as limiting values over an infinite time interval, being nonzero for chaotic orbits. Numerical approximations, computed over a finite time interval, are sometimes called "Liapunov characteristic indicators" and can be computed using the Gram-Schmidt orthogonalization technique, described by Benettin et al. (1980) and implemented by Udry & Pfenniger (1988) who kindly let us use their LIAMAG routine.

Accurate determination of the Liapunov characteristic indicators calls for integrations that extend over many orbital periods, which demands extremely long computation times, particularly when the galactic potential has a complex expression as in the first model we investigated. This fact led us to consider another technique of orbital classification that can be used both in two- and three-dimensional arbitrary potentials. It is based on the concept of spectral dynamics, introduced by Binney & Spergel (1982, 1984), using the Fourier transform of the time series of each coordinate of an orbit. Irregular orbits yield essentially a continuous spectrum, but regular orbits have basic frequencies (i.e., the frequencies of their angular variables in an action-angle representation) that can be extracted from the Fourier spectra and used to classify the regular orbit as a box, a tube, and so on. Carpintero & Aguilar (1997) prepared a code based in the method of spectral classification that allows one to classify automatically large numbers of orbits within reasonable computing times (full details can be found in their paper). A copy of their code was kindly made available to us by D. D. Carpintero.

Before going on, it is worthwhile to emphasize that, in theory, irregular and chaotic orbits are not necessarily the same. Irregular orbits have a number of isolating integrals smaller than the dimension of their configuration space and, if represented in action-angle space, they would not have a closed representation there, while chaotic orbits exhibit extreme sensitivity to initial conditions. The former can be identified by their continuous spectrum in the spectral classification method, while the latter are recognized by their nonzero Liapunov exponents. Although it can be shown that a regular orbit has vanishingly small Liapunov exponents, it has not been proved that an irregular orbit will necessarily have at least one nonzero Liapunov exponent, i.e., that it is a chaotic orbit. The generally accepted conjecture is that irregular and chaotic orbits are the same, and we will follow that trend, but it should be kept in mind that such a conjecture is not proved and that each one of the methods we used characterizes different aspects of the irregular-chaotic phenomenon. The percentages of chaotic orbits in the different models considered were obtained following a two-step approach. First, the orbits were classified as regular and irregular using the program developed by Carpintero & Aguilar (1997); in the second, and last, step, the LIAMAG routine was used to calculate the characteristic Liapunov indicators of the orbits that the spectral classification method had identified as irregular or could not classify. This procedure allowed us to make sure that these orbits were effectively chaotic and, at the same time, to estimate their characteristic Liapunov times, that is, the time needed for their chaotic nature to become apparent.

3. TRIAXIAL MODEL WITH CENTRAL PERTURBATION

To find pairs of galaxy models, comparable in density and velocity distributions but with different percentages of chaotic orbits, is not an easy task. One possibility is offered by triaxial systems, where the lack of isolating global integrals of the motion favors the presence of chaotic orbits. The abundance of this type of orbits is strongly dependent on the central density of the model, mainly because the box orbits are sensibly dependent on the form of the potential near the center (Gerhard & Binney 1985; Merritt & Fridman 1996). Thus, the percentage of chaotic orbits is very low when the model presents a smooth core (Goodman & Schwarzschild 1981), while it increases considerably in the presence of a central perturbation, such as a cusp or a black hole (Merritt & Fridman 1996; Valluri & Merritt 1998). The fact that a large part of the phase space of a triaxial potential is chaotic, particularly in models in which the gravitational force grows rapidly toward the center, and the increasing observational evidence of elliptical galaxies with central cusps or black holes (Ferrarese et al. 1994; Lauer et al. 1995), make this type of model specially attractive for the study of the effect of chaotic orbits on dynamical friction.

3.1. *Galaxy*

3.1.1. *Characteristics of the Model*

Following the studies on chaos in elliptical galaxies of Merritt & Fridman (1996) and Valluri & Merritt (1998), the galaxy inside which the satellite moves was represented by the mass model corresponding to the triaxial generalization of the spherical models of Dehnen (Dehnen 1993), which was also discussed by Tremaine et al. (1994). These models have a mass density

$$\rho(m) = \frac{(3-\gamma)M}{4\pi abc}\, m^{-\gamma}(1+m)^{-(4-\gamma)}\,, \quad 0 \le \gamma < 3\,, \quad (2)$$

with the ellipsoidal radius m defined by

$$m^2 = \frac{x^2}{a^2} + \frac{y^2}{b^2} + \frac{z^2}{c^2}\,, \quad a \ge b \ge c \ge 0\,, \quad (3)$$

and M is the total mass of the galaxy. The mass is stratified on ellipsoids with axial ratios a:b:c, where x is the long axis and z the short one. The parameter γ determines the slope of the central density cusp. For $\gamma = 0$, the model has a finite-density core; for $\gamma > 0$, the central density is infinite. These models are called *γ-models*, and the density behavior is $\rho \propto m^{-4}$ at large radii. As was mentioned in the Introduction, *Hubble Space Telescope* observations demonstrated that elliptical galaxies and bulges exhibit a variety of cusp strengths, $\gamma \le 2$. Even though few if any galaxies are observed to have $\gamma \sim 0$, we decided to use a $\gamma = 0$ model as our "basic model" ($\Phi_{(\gamma=0)}$), to assure that the box regular orbits do not turn chaotic owing to the central singularity (Gerhard & Binney 1985). Our "chaotic model" was obtained adding a central perturbation produced by a compact object (say, a black hole) to the basic model.

To represent the black hole we used a Plummer potential

$$\Phi_h(r) = -\frac{Gm_h}{\sqrt{r^2+\varepsilon_h^2}}\,, \quad (4)$$

m_h and ε_h being the mass and the softening parameter of the black hole, respectively.

The values of the total mass M, the gravitational constant G, and the x-axis scale length a were taken as unity, and those of the semiaxial ratios as $c/a = 0.5$ and $b/a = 0.79$. The expressions of the gravitational potential and the components of the force corresponding to the γ-models with $\gamma = 0$ (Merritt & Fridman 1996) were evaluated numerically using the Gaussian integration (Press et al. 1992). Following Merritt & Quinlan (1998), we adopted the maximum possible value for the black hole mass, $m_h = 0.02M$. When the mass of a central black hole exceeds roughly 2% of the mass of the host galaxy, there is a transition to global chaoticity (the boxlike orbits lose their characteristic shapes) and the galaxy responds by rapidly becoming axisymmetric. This rapid evolution may provide a negative feedback mechanism that limits the mass of nuclear black holes. The chosen value allowed us to obtain a considerable percentage of chaotic orbits with short diffusion times. It was not possible to adopt a softening parameter, ε_h, as small as the ones used by Merritt & Quinlan (1998, Table 1), however, because it would have demanded the use of extremely small integration time steps and, consequently, prohibitively long integration times, so that we adopted $\varepsilon_h = 0.08$.

3.1.2. *Initial Conditions*

The distribution function of the triaxial system considered is not known, but, as we do not need to have a self-consistent system, the initial positions and velocities of the particles that make up the galaxy were obtained from the distribution function corresponding to the spherical γ-model with $\gamma = 0$ (Dehnen 1993) and eliminating those particles that fell outside the limiting radius that contained 90% of the total mass or that were not bounded in the corresponding triaxial potential.

We used 10,000 particles in each numerical experiment. Each set of 10,000 particles was obtained from 1250 initial conditions. These conditions, following the distribution function proposed above, were generated in the whole configuration space (including the eight octants). Then the position of each particles was projected in the seven remaining octants of the space (the octants that do not host the particles initially), obtaining seven new particles from each of the original 1250 ones. The velocities of these new seven particles were chosen so as to have moduli equal to the one of the original particle and with their Cartesian components assigned so as to have the same orbit for all the eight particles but with opposite directions. This procedure presents two advantages. On the one hand, it guarantees that, initially, the center of mass of the galaxy is at the origin of the potential and that the system has no net angular momentum. On the other hand, it allows us to estimate the percentage of chaotic orbits present in the models considered from the analysis of one-eighth of the particles that make up the galaxy only, saving computing time. Using different seed numbers, we created three pairs of models, each one having the basic model ($\Phi_{(\gamma=0)}$), and the chaotic model ($\Phi_{(\gamma=0)} + \Phi_h$).

Starting with those initial conditions, the equations of motion of the particles were integrated, for a few orbital periods, in the potentials $\Phi_{(\gamma=0)}$ and $\Phi_{(\gamma=0)} + \Phi_h$, allowing them to mix in the potential that represents the galaxy in each case. The density and velocity distributions were obtained in order to check whether there were any significant differences between the basic and perturbed models. Both distributions were derived considering the masses contained in spherical shells with equal numbers of particles, and, although this method ignores the triaxiality of the models, it is enough for comparing them. The density distribution turned out to be very similar for both models, and the anisotropy parameter $\beta(r)$ (Binney & Tremaine 1987) is $\simeq 0$, so that the velocity distribution is in both cases isotropic. Another quantity that can modify the effect of the dynamical friction is the velocity dispersion. This topic was studied by Wahde et al. (1996) for disk galaxies, using non–self-consistent simulations. They found that the velocity dispersion has a very small influence on this process. Analyzing the velocity dispersion in our case, we observed that it does not change during the evolution of the system and that its distribution is very similar in nonperturbed and perturbed models, finding a good agreement between two- and three-dimensional results. Therefore, we can safely assume that any differences that might arise between the satellite orbital decays in each model can be attributed to the difference in the percentages of chaotic orbits.

3.1.3. *Results of the Orbital Classification*

Our next step, following the scheme of orbital classification described in § 2, was to use the program of spectral analysis to classify the orbits of the particles in the three pairs of models we had created. The results of the analysis

TABLE 1

RESULTS OF THE SPECTRAL ANALYSIS OF THE TRIAXIAL GENERALIZATION OF THE γ-MODEL WITH $\gamma = 0$ WITHOUT AND WITH CENTRAL PERTURBATION (IN PERCENT)

	GALAXY 1		GALAXY 2		GALAXY 3	
TYPE OF ORBITS	$(\Phi_{\gamma=0})$	$(\Phi_{\gamma=0} + \Phi_h)$	$(\Phi_{\gamma=0})$	$(\Phi_{\gamma=0} + \Phi_h)$	$(\Phi_{\gamma=0})$	$(\Phi_{\gamma=0} + \Phi_h)$
Box	16.9	7.0	16.9	7.0	17.3	6.9
x-tube.....	25.4	26.5	27.6	29.0	25.9	27.0
y-tube.....	0.1	0.0	0.1	0.0	0.0	0.0
z-tube	46.6	47.4	44.3	46.6	44.6	45.5
Irregular.....	11.0	19.1	11.1	17.4	12.2	20.6

for each component of the three pairs of models (dubbed *galaxy 1*, *galaxy 2*, and *galaxy 3*, respectively) are given in Table 1, as the percentages of regular orbits (discriminating between box and tube orbits) and the percentages of irregular orbits (including those that could not be classified, because our previous experience with this method indicates that most of them turn out to be irregular).

As expected, the percentages of irregular orbits in the chaotic models grow at the expense of the box orbits of the corresponding regular model in all three cases, in agreement with previous results (Gerhard & Binney 1985; Merritt & Fridman 1996).

The orbital classification was completed computing the Liapunov characteristic exponents of the orbits revealed as irregular in the previous step for galaxy 1. We took advantage of the knowledge of the periods obtained from the spectral analysis to integrate the orbits for about 10^3 orbital periods, an interval long enough for the computed Liapunov characteristic indicators to level close to their true value (for an infinite time interval). It turned out that the greatest Liapunov indicator, σ_1, ranged between $\sigma_1 \simeq 9 \times 10^{-5}$ and 1.5×10^{-2} in the basic model and between $\sigma_1 \simeq 2 \times 10^{-4}$ and 5×10^{-2} in the chaotic model, as shown in Figure 1.

The timescale required by the chaotic orbits to experience an exponential divergence is given by the Liapunov time, which is defined as the inverse of the greatest Liapunov exponent. For very low values of σ_1, the Liapunov times are so large that the corresponding chaotic orbit behaves as regular during timescales of astronomical interest (Goodman & Schwarzschild 1981). In the present study, it is crucial to have orbits with Liapunov times well below the time that the satellite needs to reach the center of the galaxy, which we refer to as the "decay time." This is necessary to ensure that chaotic orbits behave as such during the orbital decay of the satellite, in order to estimate the effect of chaotic orbits on dynamical friction. The time when the satellite starts to show a marked energy loss, as a consequence of its interaction with the particles of the galaxy, is referred to as the "critical time" and can be obtained from the results of the numerical experiments on satellite decay that will be described later. We assumed that the chaotic orbits that affected the orbital decay of the satellite were those orbits that had Liapunov times shorter than this critical time.

3.2. *Satellite*

The satellite was modeled as an extended object represented by a softened point mass. We adopted a satellite mass $m_s = 0.01M$, larger than the masses of the particles that made up the galaxy, and a scale length parameter ε_s given by the expression (CMV)

$$\varepsilon_s = \varepsilon\sqrt{m_s}\ , \tag{5}$$

where ε is the scale length parameter of the galaxy, that in this case coincides with the x-axis scale length $a(=1)$.

The initial conditions were chosen so as to get orbital decay times larger than the Liapunov times of most of the

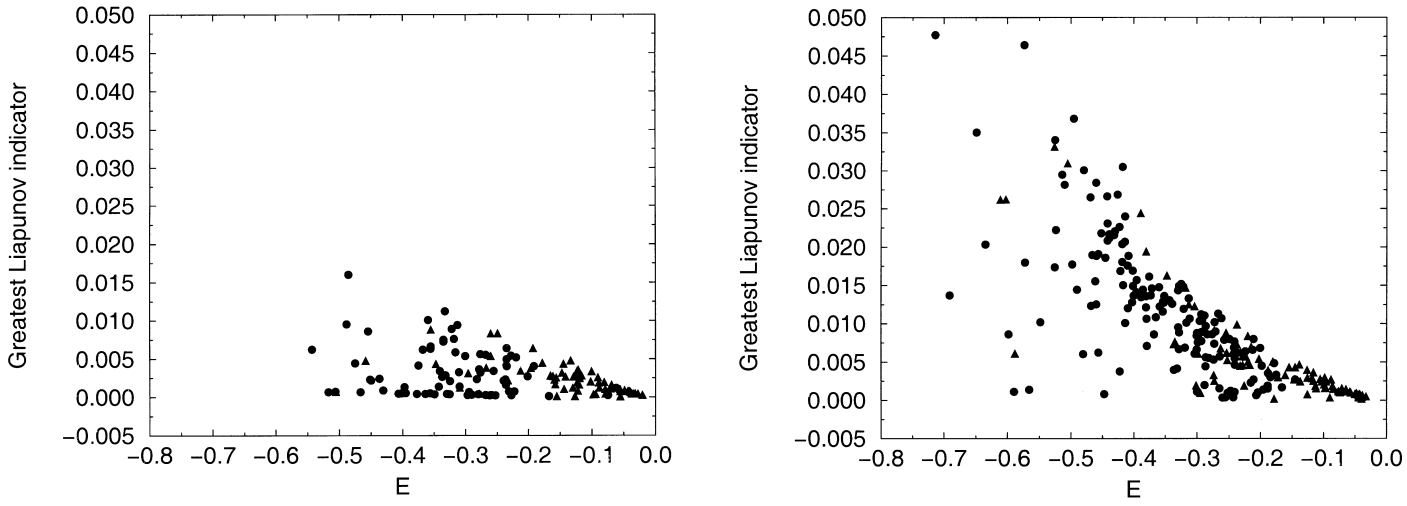

FIG. 1.—Largest Liapunov characteristic indicators, σ_1, of each orbit as a function of its energy for the triaxial generalization of the γ-model with $\gamma = 0$ (galaxy 1) without and with central perturbation: basic model (*left*), and chaotic model (*right*). The circles identify the orbits classified as irregular by the spectral analysis method, and the triangles identify the nonclassified orbits.

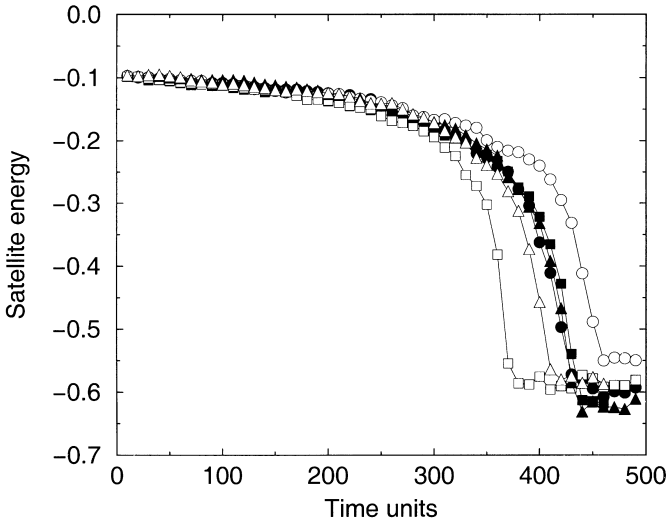

FIG. 2.—Evolution of the energy of the satellite with respect to the galaxy (represented by the triaxial generalization of the γ-model with $\gamma = 0$) for the basic models (*empty symbols*) and the chaotic models (*filled symbols*). Each pair of models is identified by a different type of symbol: circle for galaxy 1, square for galaxy 2, and upward-pointing triangle for galaxy 3.

orbits classified as chaotic in the perturbed model. From Figure 1 (*right-hand plot*), it seems reasonable to discard those orbits with values of σ_1 smaller than 2.5×10^{-3}, which means that the bulk of the Liapunov times are shorter than 400 time units. The selected initial position of the satellite corresponds to a distance of approximately 1.6 times the half-mass radius of the galaxy. Its initial velocity was chosen so as to have a circular orbit in Dehnen's spherical model with $\gamma = 0$, the simplest one we could consider to analyze the process under investigation.

3.3. *Numerical Experiments*

The numerical integrations were performed with a non–self-consistent code, with the equations of motion given by equation (1), where the potential Φ is $\Phi_{\gamma=0}$ or $\Phi_{\gamma=0} + \Phi_h$.

The effect of the compact object at the center of the galaxy was included in the equations of motion of the particles that make up the galaxy, but not in those of the satellite. In that way, were it not for the particle-satellite interactions, the orbit of the satellite would be the same in the basic and the chaotic models; any departure can then be attributed to the different sort of orbits (regular or chaotic) used in each model.

3.4. *Orbital Decay*

The time used by the satellite to reach the center of the galaxy ranged from 375 to 450 time units, approximately, and the final integration time (500 time units) was chosen so as to allow the orbit of the satellite to decay completely.

TABLE 2

RESULTS OF THE ORBITAL CLASSIFICATION CORRESPONDING TO A PAIR OF TRIAXIAL γ-MODELS OBTAINED FROM GALAXY 1 (IN PERCENT)

Type of Orbits	$(\Phi_{\gamma=0})$	$(\Phi_{\gamma=0} + \Phi_h)$
Chaotic ($T_{\rm Lia} \leq 300$ t.u.).....	3.7	13.7
Chaotic (300 t.u. $< T_{\rm Lia} <$ 400 t.u.).....	1.2	1.1
Chaotic ($T_{\rm Lia} \geq 400$ t.u.) + regular	95.1	85.2

These values are long enough to allow the chaotic orbits with Liapunov times shorter than 400 time units, which are the majority, to show exponential divergence during the orbital decay of the satellite. The percentages of chaotic orbits that affect the satellite are given in § 3.5.

The orbital decay of the satellite was followed through the time evolution of the total energy of the satellite with respect to the galaxy. Figure 2 compares the energy loss of the satellite in the basic and chaotic models. It has to be noted that from the evolution of the Lagrangian radius, as the satellite decays, we also observed that there is not a structural change for the basic model. The chaotic model does show a slight expansion with respect to the regular model (more pronounced in the outer shells), but it occurs only after the satellite reaches the galactic center, not affecting the orbital decay.

Taking as the decay time the time needed for the satellite to reach an energy of -0.5, we obtained the mean values $\langle t \rangle_b$ and $\langle t \rangle_c$ for the basic and chaotic models, respectively, with their corresponding standard deviations

$$\langle t \rangle_b = 407.53 \pm 24.6 \text{ and } \langle t \rangle_c = 423.2 \pm 1.78 .$$

These quantities indicate that the difference between these values is not significant and that it is well below the combined 3 σ level. The large difference between the standard deviations obtained for the basic and chaotic models is probably not significant and due to the small samples used.

3.5. *Chaotic Orbits that Might Affect the Orbital Decay*

From the analysis of the 1250 orbits initially generated for galaxy 1, we obtained, for the basic and chaotic models, the percentage of orbits considered chaotic with Liapunov times shorter than the critical time. This time, estimated as 300 time units, corresponds to the time when the satellite begins to experiment the greatest energy loss. We also determined the percentage of chaotic orbits with Liapunov times longer than the critical time, but shorter than the orbital decay time (400 time units, on average; see Fig. 2). These values are shown in Table 2.

We see from the table that the percentage of chaotic orbits with $T_{\rm Lia} \lesssim 300$ time units in the chaotic model is almost 4 times larger than the corresponding percentage in the basic model, while the equivalent ratio for irregular orbits from Table 1 is less than 2. Nevertheless, all those percentages are small, and the similarity between the decay times of both models may be attributed to the lack of a large number of chaotic orbits in the chaotic model. Therefore, in the next section we examine another kind of model that yields larger fractions of chaotic orbits than the case considered here.

4. TRIAXIAL MODEL WITH ROTATION

Another way of perturbing a slightly nonintegrable triaxial model so as to increase the chaoticity is to place the system on a circular orbit in a background potential; the perturbed model will be referred to as the "rotating model." The motivation for using such a model comes from the work of CMV, who classified the orbits found in a modified Satoh potential (see Satoh 1980 for the original Satoh model) that, in turn, moved on a circular orbit in a logarithmic potential. Even though CMW analyzed only the orbits in a model with rotation, finding that it has a large number of chaotic orbits, it is reasonable to expect that the orbits in the static modified Satoh potential are mostly regular,

owing to the close resemblance of this potential to the Plummer potential. This assumption was corroborated in the present study; the results are described in § 4.1.3.

4.1. *Galaxy*

4.1.1. *Characteristics of the Model*

Following CMW, we represented the galaxy in our new basic model with a modified Satoh potential

$$\Phi_S(x, y, z) = -\frac{GM}{\sqrt{x^2 + y^2 + z^2 + g\{g + 2[y^2 + (z/b)^2 + h^2]^{1/2}\}}}, \quad (6)$$

where G is the gravitational constant and M is the total mass of the galaxy, both taken as unity. The values assigned to the form parameters are $b = 0.8$, $h = 0.5$, and $g = 0.05$ (according to CMW), which yield moderately triaxial equipotential curves. The profiles along the x-, y- and z-axes of the modified Satoh potential are shown in Figure 3 (*left-hand plot*).

The rotating model was obtained letting the galaxy move on a circular orbit around the center of a background potential (logarithmic potential)

$$\Phi_L(x, y, z) = \tfrac{1}{2}\omega^2 R^2 \ln[(R + x)^2 + y^2 + z^2], \quad (7)$$

ω being the angular velocity of the rotating system, and R the radius of its orbit; following CMW, their values were taken as 0.5 and 100, respectively.

As the galaxy moves on the circular orbit, the x-axis points in the direction opposite to the center of the logarithmic potential, the y-axis lies in the direction of the orbital motion, and the z-axis is perpendicular to the orbital plane. The equations of motion are given by CMW. The effective potential of the rotating model is

$$\Phi_{ef}(x, y, z) = \Phi(x, y, z) - \tfrac{1}{2}\omega^2[(R + x)^2 + y^2 - R^2], \quad (8)$$

where the second term corresponds to the contribution of the centrifugal energy, and the first term is the sum of the galaxy potential, Φ_S, and the background potential, Φ_L. Figure 3 (*right-hand plot*) shows the corresponding effective potential profiles along x-, y-, and z-axes (notice that the effective potential is not exactly symmetric in the x-direction). We notice that rotation enhances considerably the triaxiality of the equipotentials.

4.1.2. *Initial Conditions*

Since the distribution function corresponding to the chosen potential is unknown, we generated the initial conditions in a way similar to the one we used for the triaxial generalization of Dehnen's spherical model. We started with the Plummer potential (Binney & Tremaine 1987)

$$\Phi(r) = -\frac{GM}{\sqrt{\varepsilon^2 + r^2}}, \quad (9)$$

whose distribution function is known. The scale factor ε was chosen so that the values of the Plummer and the modified Satoh potentials coincided at the origin ($\varepsilon = 0.229$, for the adopted values of the constants g and h).

To have all the particles bounded, we truncated the mass distribution at the limiting radius that comprises 94% of the total mass of the galaxy ($r_l = 1.1165$); in this way, all the generated particles had energies lower than $E_l = -1.1878$, and the half-mass radius turned out to be $r_{1/2} \simeq 0.3$.

The equations of motion are easier to integrate than in the triaxial generalization of Dehnen's spherical model, and we were able to consider galaxies with a larger number of particles. Following the process described in § 3.1.2, we obtained two sets of galaxies with isotropic velocity distribution, one consisting of five galaxies of 50,000 particles each, and another with three galaxies of 10,000 particles each. For each galaxy, in turn, we had a pair of models: the basic (Φ_S), and the rotating (Φ_{ef}) models. The density and velocity distributions (and, thus, the velocity dispersion) were essentially the same in both types of models, so that any differences that might arise between the orbital decay times of the satellite can be safely attributed to the effect of the different percentages of chaotic orbits present in each model.

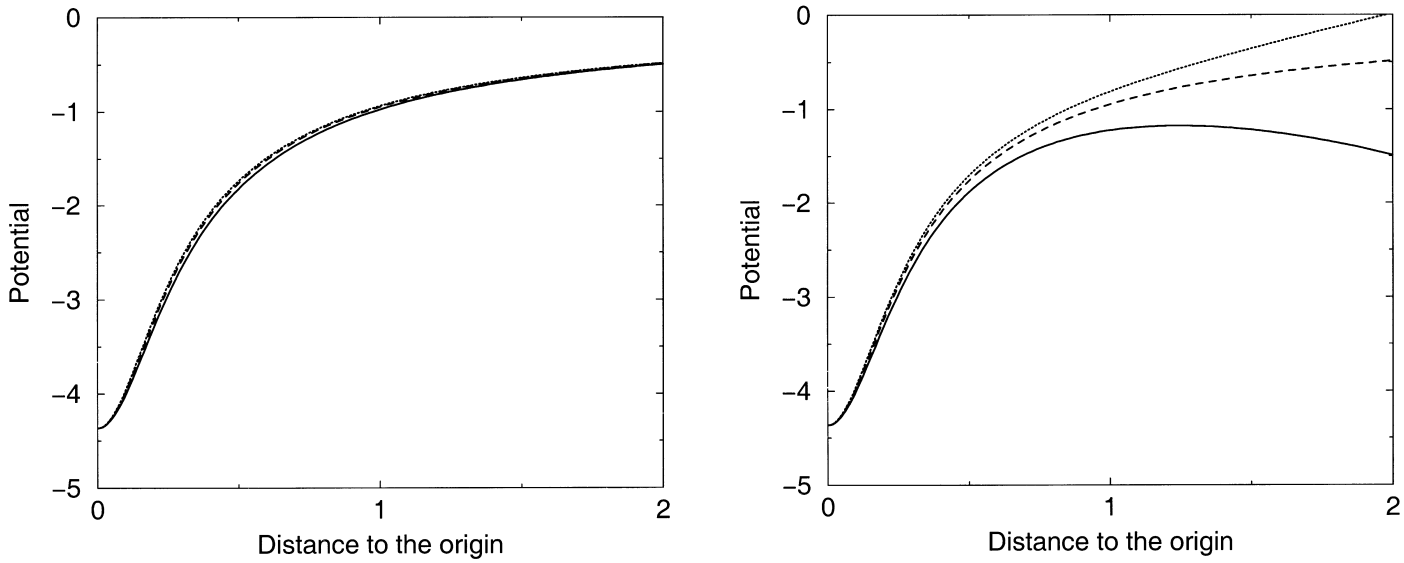

FIG. 3.—Potential profiles along the x-axis (*full line*), y-axis (*dashed line*), and z-axis (*dotted line*) of the modified Satoh potential without rotation (basic model [*left*]) and with rotation (chaotic model [*right*]).

4.1.3. *Orbital Classification*

The orbital classification was performed as indicated in § 2, analyzing only one-eighth of the particles contained in the galaxies made up of 50,000 particles.

Our results of the spectral analysis are given in Table 3 where, as in Table 1, orbits grouped under the name of "irregular" include those classified as irregular as well as those that could not be classified by the automatic code.

The mild triaxiality of the basic model gives rise to a very small percentage of chaotic orbits. When rotation is introduced, the percentage of box orbits is only slightly affected, but the percentages of tube orbits are significantly altered and the number of chaotic orbits increases at their expense. Table 3 shows that the x-tube orbits practically disappear in the rotating model, while the number of z-tube orbits increases about 10% and the amount of y-tube orbits is negligibly small throughout.

Muzzio et al. (2000a, 2000b) have discussed the origin of chaoticity in these rotating models. Suffice it here to say that it seems to be due to an interplay of three forces: the attractive force of the galaxy, the differential centripetal-centrifugal force, and the Coriolis force; the triaxiality of the model, although causing little chaoticity on its own, substantially increases it when combined with rotation.

We computed the Liapunov characteristic indicators for the irregular and nonclassified orbits of galaxy 1. These orbits were integrated for longer times (10^4 orbital periods) than those we had used for the γ-model with central perturbation. The results showed that the values of the greatest Liapunov indicator, σ_1, ranged between 3×10^{-4} and 5×10^{-2} for the basic model and between 3×10^{-4} and 1.8×10^{-1} for the chaotic model, approximately. Figure 4 shows the values corresponding to galaxy 1 as a function of the energy of each particle for the two models.

While the Liapunov indicators confirm that the bulk of these orbits is chaotic, we will return to them later to discuss how long does it take to these orbits to exhibit their exponential divergence.

4.2. *Satellite*

The larger number of particles that make up these galaxies allowed us to use less massive satellites, thus obtaining more realistic conditions. Therefore, we simulated our satellites with Plummer models having the following parameters

$$\varepsilon_s = 0.01 \text{ for } m_s = 0.002 ,$$

$$\varepsilon_s = 0.0229 \text{ for } m_s = 0.01 .$$

The initial positions of the satellite were chosen so as to obtain decay times longer than the Liapunov times of the bulk of the chaotic orbits of the particles in the galaxy. Since dynamical friction is proportional to the mass of the satellite, the less massive satellite should start closer to the galactic center than the more massive one. Therefore, we adopted as initial positions for the satellites with $m_s = 0.002$ and 0.01 the radii that contained 85% and 88% of the total mass of the Plummer model with $\varepsilon = 0.229$, respectively. These values are inside the x-axis potential turnover, and a slight

TABLE 3

RESULTS OF THE SPECTRAL ANALYSIS OF THE MODIFIED SATOH MODEL WITHOUT AND WITH ROTATION (IN PERCENT)

	GALAXY 1		GALAXY 2		GALAXY 3		GALAXY 4		GALAXY 5	
TYPE OF ORBITS	(Φ_S)	(Φ_{ef})	(Φ_S)	(Φ_{ef})	(Φ_S)	(Φ_{ef})	(Φ_S)	(Φ_{ef})	(Φ_S)	(Φ_{ef})
Box	15.6	13.8	15.9	13.6	15.5	12.2	15.5	13.4	15.3	13.6
x-tube.....	46.4	0.8	46.6	0.8	47.9	0.5	47.0	0.7	47.2	0.3
y-tube.....	0.0	0.1	0.0	0.1	0.0	0.0	0.0	0.0	0.1	0.1
z-tube.....	37.2	46.6	36.3	46.9	35.6	48.1	36.5	47.2	36.3	47.8
Irregular.....	0.8	38.7	1.2	38.6	1.0	39.1	1.0	38.7	1.1	38.2

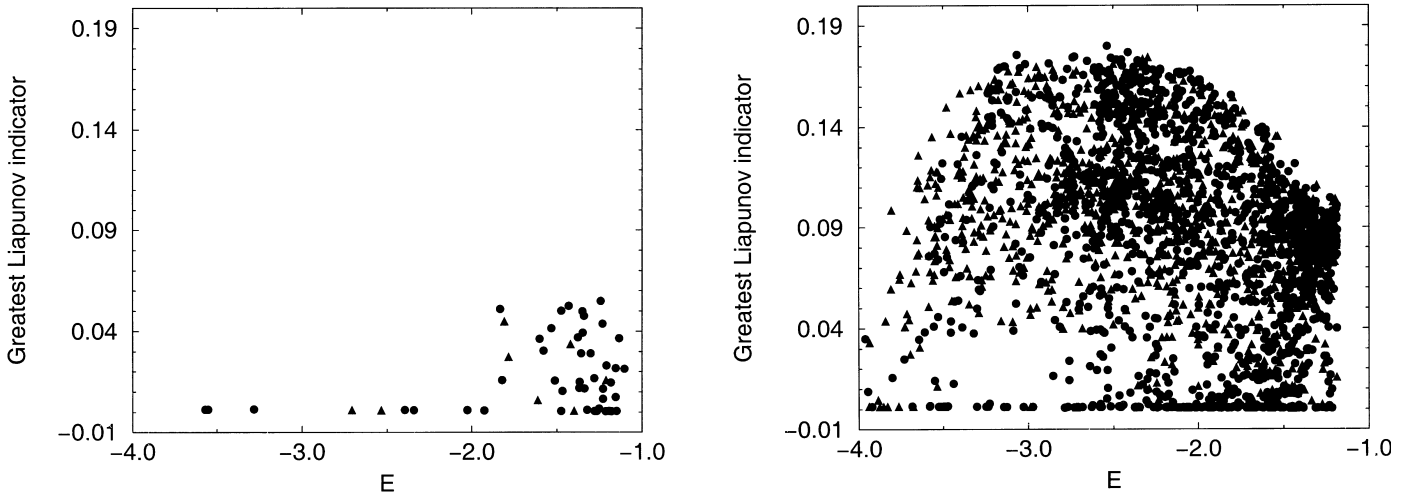

FIG. 4.—Liapunov greatest indicator, σ_1, for each particle as a function of the particle energy for the modified Satoh model (galaxy 1) without and with rotation: basic model (*left*), and chaotic model (*right*). The circles identify the orbits classified as irregular by the method of spectral analysis, and the triangles identify the nonclassified orbits.

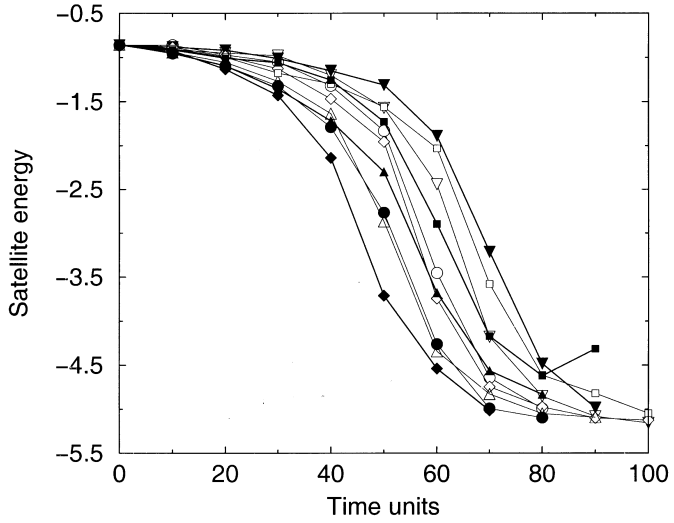

FIG. 5.—Total energy of the satellite with respect to the galaxy (represented by the modified Satoh model) as a function of the integration time corresponding to the simulations with $N = 50{,}000$ and $m_s = 0.002$. The empty and filled symbols identify the orbital decays corresponding to the basic models and the chaotic models, respectively. Each pair of model is distinguished by different symbols: circle for galaxy 1, downward-pointing triangle down for galaxy 2, diamond for galaxy 3, upward-pointing triangle up for galaxy 4, and square for galaxy 5.

TABLE 4

MEAN VALUES OF THE ORBITAL DECAY TIMES FOR THE THREE GROUPS OF SIMULATIONS WITH THE SATOH MODIFIED GALAXY MODEL

Type of Orbits	(Φ_S)	(Φ_{ef})
Group I:		
$N = 50{,}000$	$\langle t\rangle_r = 61.79 \pm 2.7$	$\langle t\rangle_c = 59.84 \pm 4.05$
$m_s = 0.002$		
Group II:		
$N = 50{,}000$	$\langle t\rangle_r = 26.63 \pm 0.99$	$\langle t\rangle_c = 26.0 \pm 1.5$
$m_s = 0.01$		
Group III:		
$N = 10{,}000$	$\langle t\rangle_r = 28.45 \pm 2.28$	$\langle t\rangle_c = 24.75 \pm 1.84$
$m_s = 0.01$		

TABLE 5

RESULTS OF THE ORBITAL CLASSIFICATION CORRESPONDING TO A PAIR OF MODIFIED SATOH MODELS OF GROUP I (IN PERCENT)

Type of Orbits	(Φ_S)	(Φ_{ef})
Chaotic ($T_{Lia} \leq 20$ t.u.)	0.1	30.9
Chaotic (20 t.u. $< T_{Lia} <$ 60 t.u.).....	0.3	3.7
Chaotic ($T_{Lia} \geq 60$ t.u.) + regular.....	99.6	65.4

difference in the initial radius makes a great difference in the decay times.

In order that the satellite gets an approximately circular orbit, we gave to it a purely tangential velocity equal to that needed to obtain a circular orbit in the Plummer model that mimics the central part of the Satoh potential (i.e., $\varepsilon = 0.229$).

4.3. *Numerical Experiments*

We performed three sets of numerical experiments, changing the number of particles in the galaxy and the mass of the satellite. Each set consisted of pairs of numerical simulations with equal initial conditions for the galaxy, but the galaxy was represented in one case by the basic model, Φ_S, and in the other by the chaotic model, Φ_{ef}. The equations of motion of the satellite were the same in both cases, so that the satellite did not feel the effect of the rotation and any change in its orbital decay can be attributed to the effect of the chaotic orbits only.

In group I, which includes five pairs of simulations, we considered a galaxy made up of 50,000 particles and the least massive satellite ($m_s = 0.002$). Groups II and III include three pairs of numerical experiments, which simulate the orbital decay of the most massive satellite ($m_s = 0.01$) within galaxies made up of 50,000 and 10,000 particles, respectively.

The satellites reach the center of the galaxy in less than 100 time units for the group I models and in less than 50 time units for the groups II and III models, so that those intervals were chosen for the corresponding total integration times. Figure 4 shows that there are few orbits with σ_1

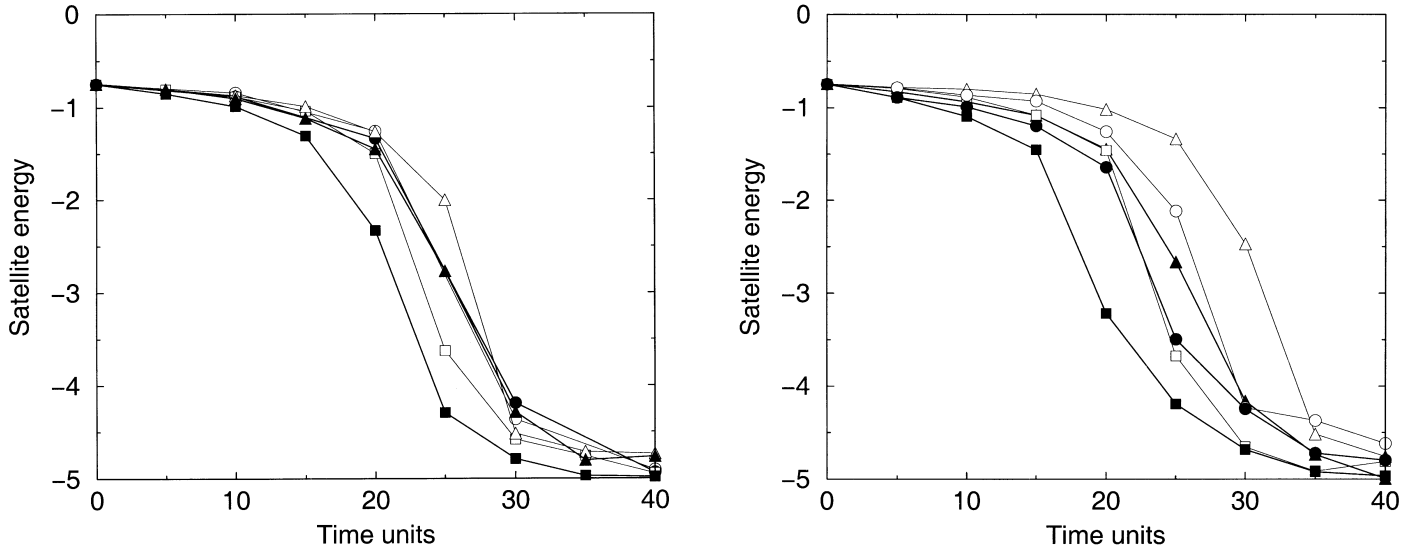

FIG. 6.—Total energy of the satellite with respect to the galaxy (represented by the modified Satoh model) as a function of the integration time corresponding to the simulations with $N = 50{,}000$ and $m_s = 0.01$ (*left*) and $N = 10{,}000$ and $m_s = 0.01$ (*right*). Each pair of model is distinguished by different symbols. The empty and filled symbols identify the orbital decays corresponding to the basic models and the chaotic models, respectively.

values smaller than 0.02 (i.e., Liapunov times longer than 50 time units), and, consequently, most of the particles have timescales of exponential divergence shorter than the orbital decay times.

4.4. *Results*

Figures 5 and 6 show the orbital decay of the satellite for each group of simulations.

Although the basic and chaotic models have similar density and velocity distributions, the perturbation caused by the rotation might alter the structure of the chaotic model. Therefore, in order to ensure that differences in the decay times arose only from the different chaoticity, we followed the evolution of the radii that contained different percentages of the mass of the galaxy for the two types of models. Again, our results showed that the global structure of the galaxy for the basic and chaotic models remained unaffected during the orbital decay of the satellite.

The satellite decay time was adopted as the time when the satellite reaches an energy $E_{\rm sat} = -3.5$. Table 4 gives the mean values of these times ($\langle t \rangle_b$ and $\langle t \rangle_c$ for the basic models and the chaotic models, respectively, with their corresponding standard deviations).

Figures 5 and 6 and the values of Table 4 strongly suggest that chaoticity has no significant effect on the orbital decay of the satellites. Nevertheless, before reaching conclusions, it seems advisable to check the numbers of chaotic orbits that behave as such in timescales shorter than the satellite decay times.

4.5. *Chaotic Orbits that Might Affect the Orbital Decay*

Repeating the analysis performed in § 3.5, Table 5 shows the percentages of orbits with regular and chaotic behavior, obtained from the 6250 particles initially analyzed in the basic and chaotic models of group I.

The chaoticity of the modified Satoh model is greatly enhanced by rotation, as can be seen from Table 5. This table also shows that the bulk of the orbits manifest their exponential divergence in timescales shorter than about 20 time units, i.e., an interval after which the satellite begins to suffer an important energy loss. These results, plus the fact that it does not exist any significant difference between the orbital decay times in the basic and the chaotic models, let us conclude that dynamical friction is not affected by the presence of chaotic orbits.

5. DISCUSSION

The need to investigate the effect of chaotic orbits on dynamical friction arose, on the one hand, from the increasing recognition of the relevance of chaos in many stellar systems and, on the other hand, from the very interesting, but limited, suggestion of Pfenniger (1986).

The results obtained with the triaxial Dehnen model were not conclusive because, even in the cases with a central compact object, the percentages of chaotic orbits were low. Nevertheless, those experiments are significant because, if chaoticity affected relaxation times by orders of magnitude, as Pfenniger had suggested, and dynamical friction were similarly altered, even with that low chaoticity, they should have shown some difference in the orbital decay rates.

The difficulty in finding a pair of models with similar density and velocity distributions, but with different percentages of chaotic orbits, had not been recognized by us initially and proved to be quite a challenge. The investigation of CMW was extremely useful in solving this problem, and, although the resulting system may be rather artificial, it turned out to be very adequate to isolate the effect we were interested in. In this case, the difference in chaoticity between the models with and without rotation is very important, and, moreover, as the bulk of the orbits have Liapunov times shorter than the satellite decay times, the exponential sensitivity of the dynamics has enough time to manifest itself. Therefore, the results obtained from those models allow us to safely decide that there is no significant effect of the chaoticity on dynamical friction.

Let us conclude with some speculation on how our results can be reconciled with those of Pfenniger. We recall, first of all, that Pfenniger centered his discussion on the relaxation time and that he referred to the possible change in dynamical friction only as a consequence of the change in the relaxation time that he thought could be induced by the chaoticity. We will center, instead, on dynamical friction, which is a local phenomenon (Cora et al. 1997) and, as assumed by Chandrasekhar (1943), can be regarded as the result of the sum of the small effects of numerous individual two-body interactions (the satellite and the stars of the galaxy that the satellite encounters in its way). Now, the exponential divergence of the chaotic orbits means that small departures from initial positions or velocities lead to differences in the coordinates and velocities that grow exponentially with time, so that a tiny initial difference will remain small at first and will grow appreciably only after an interval of time of the order of the Liapunov time. The encounter of the satellite with an star moving on a chaotic orbit may be considered, as Chandrasekhar did, as an isolated two-body problem: the interaction is important only while the distance between the satellite and the star is short so that, on the one hand, the tidal effects are negligible and, on the other hand, the encounter lasts a very short time (some orders of magnitude less than the orbital period). Therefore, what happens during the encounter has nothing to do with the orbits of both the satellite and the star because, in the center of mass of the system they make up, everything happens as an interaction of two bodies governed by Newton's law. The changes suffered by the satellite will depend only on the positions and velocities that the satellite and the stars have when they enter the "region of encounter"; consequently, as long as the density and velocity distributions in the galaxy are the same, there is no reason for the dynamical friction to experience any variation, just as the results of our experiments show. Of course, the dynamics of the star will be very different after an encounter with the satellite, depending on whether it moves on a regular or chaotic orbit; while the former will not be greatly affected, the latter will depart considerably from the original orbit. In other words, even though we checked carefully that chaotic orbits had Liapunov times comparable with the satellite decay time, we can see now that this time is not the most important one: for dynamical friction to be affected by the presence of chaotic orbits, Liapunov times should be of the order of the time over which an encounter extends, that is, orders of magnitude shorter than the orbital period. Such possibility seems to be well beyond, not only of the reality of stellar systems but also from its control through numerical experiments (even if they were extremely artificial).

Chandrasekhar (1943) found the relationship between dynamical friction and relaxation time (also included in

Pfenniger 1986 as his formula [2]), so that the previous discussion could, in principle, be equally done in terms of the relaxation time rather than in terms of the dynamical friction. The problem is that, from the point of view of the relaxation time (adopted by Pfenniger), the situation is much less clear than from the point of view of the dynamical friction (adopted above). The relaxation time is generally defined as the time that a system takes to return to equilibrium after it was taken out of it. In stellar dynamics it is usually understood as the time a star needs to alter significantly its velocity as a result of encounters with other stars. In this sense, it is clear that the result will be very different depending on whether the star moves on a regular orbit or on a chaotic one. In the first case, the departures from the original orbit will be produced only by the cumulative effects of the encounters, while, in the second one, to the foregoing effect the exponential divergence of the orbits should be added. Obviously, the first effect is related to the star-star interactions, while the second one depends only on the characteristics of the potential. Let us imagine an ideal case in which a star moving on a chaotic orbit suffers an encounter with another star at intervals of time of the order of the Liapunov time of its orbit. With such long-spaced encounters, the collisional relaxation time will be very much longer than the corresponding Liapunov time, but the orbit would suffer appreciable changes in its velocity in intervals of the order of the Liapunov time, which will then become the relaxation time, according to the definition. The important point to stress here is that this relaxation time would have nothing to do with the collisional process: there would be a wide range in which the density and velocity distributions of the stars could change, without altering this relaxation time; furthermore, the appreciable changes in the velocity of the star on the chaotic orbit could result from other, noncollisional, phenomena (such as slight fluctuations in the potential, for example). In our opinion, the problem of Pfenniger's work is that it does not distinguish between these two processes, one related to the stellar encounters and the other to the characteristics of the potential, concentrating only on the changes suffered by the orbit.

For a long time, consciously or unconsciously, the ideas of linearity and regularity have dominated the thoughts of the stellar dynamicists. If chaos turns out to be important in some stellar systems, as recent investigations are suggesting, many concepts (such as relaxation time), which are precise and clear in a context of regularity, will need to be redefined to be applicable to chaotic situations.

We thank J. A. Núñez and D. D. Carpintero for useful discussions and P. M. Cincotta for helpful correspondence. We also thank D. Pfenniger and D. D. Carpintero for kindly making available their codes. We are grateful to S. D. Abal, M. C. Fanjul de Correbo, R. E. Martínez, E. Suárez, and R. H. Viturro for their technical assistance. This work was supported by grants from the Universidad Nacional de La Plata and from the Consejo Nacional de Investigaciones Científicas y Técnicas de la República Argentina.

REFERENCES

Athanassoula, E., Bienaymé, O., Martinet, L., & Pfenniger, D. 1983, A&A, 127, 349
Bennetin, G., Galgani, L., Giorgilli, A., & Strlcyn, J. M. 1980, Meccanica, 15, 21
Binney, J., & Spergel, D. 1982, ApJ, 252, 380
———. 1984, MNRAS, 206, 159
Binney, J., & Tremaine, S. 1987, Galactic Dynamics (Princeton: Princeton Univ. Press)
Bontekoe, Tj. R., & van Albada, T. S. 1987, MNRAS, 224, 349
Borne, K. D. 1984, ApJ, 287, 503
Carpintero, D. D., & Aguilar, L. A. 1997, MNRAS, 298, 1
Carpintero, D. D., Muzzio, J. C., & Wachlin, F. C. 1999, Celest. Mech. Dyn. Astron., 73, 159 (CMW)
Chandrasekhar, S. 1943, ApJ, 97, 255
Colpi, M., Mayer, L., & Governato, F. 1999, ApJ, 525, 720
Contopoulos, G. 1983, A&A, 117, 89
Contopoulos, G., & Grosbol, P. 1989, Astron. Astrophys. Rev., 1, 261
Contopuolos, G., & Papayannopoulos, T. 1980, A&A, 92, 33
Cora, S. A., Muzzio, J. C., & Vergne, M. M. 1997, MNRAS, 289, 253 (CMV)
Crane, P., et al. 1993, AJ, 106, 1371
Dehnen, W. 1993, MNRAS, 265, 250
Ferrarese, L., van den Bosch, F. C., Ford, H. C., Jaffe, W., & O'Connell, R. W. 1994, AJ, 108, 1598
Ford, H. C., et al. 1994, ApJ, 435, L27
Gerhard, O. E., & Binney, J. J. 1985, MNRAS, 216, 467
Goodman, J., & Schwarzschild, M. 1981, ApJ, 245, 1087
Hernquist, L., & Weinberg, M. D. 1989, MNRAS, 238, 407
Jaffe, W., Ford, H. C., O'Connell, R. W., van den Bosch, F. C., & Ferrarese, L. 1994, AJ, 108, 1567
Lauer, T. R., Ajhar, E. A., Byun, Y., Dressler, A., Faber, S. M., Grillmair, C., Kormendy, J., & Richstone, D. 1995, AJ, 110, 1622
Lichtenberg, A., & Lieberman, M. 1992, Regular and Chaotic Dynamics (2d ed.; New York: Springer)
Merritt, D., & Fridman, T. 1996, ApJ, 460, 136
Merritt, D., & Quinlan, G. 1998, ApJ, 498, 625
Miyoshi, M., et al. 1995, Nature, 373, 127
Muzzio, J. C., Carpintero, D. D., & Wachlin, F. 2000a, Adv. Ser. in Astrophys. and Cosmology, 10, 107
Muzzio, J. C., Wachlin, F., & Carpintero, D. D. 2000b, in IAU Colloq. 174, Small Galaxy Groups, ed. M. J. Valtonen & C. Flynn (ASP Conf. Ser. 209; San Francisco: ASP), 281
Pfenniger, D. 1984, A&A, 141, 171
———. 1986, A&A, 165, 74
Press, W. H., Vetterling, S. A., Teukolsky, S. A., & Flannery, B. P. 1992, Numerical Recipes in Fortran (2d ed.; Cambridge: Cambridge Univ. Press)
Prugniel, Ph., & Combes, F. 1992, A&A, 259, 25
Satoh, C. 1980, PASJ, 32, 41
Séguin, P., & Dupraz, C. 1994, A&A, 190, 709
———. 1996, A&A, 310, 757
Tremaine, S., Richstone, D., Buyn, Y. I., Dressler, A., Faber, S. M., Grillmair, C., Kormendy, J., & Lauer, T. R. 1994, AJ, 107, 634
Tremaine, S., & Weinberg, M. D. 1984, MNRAS, 209, 729
Udry, S., & Pfenniger, D. 1988, A&A, 198, 135
Valluri, M., & Merritt, D. 1998, ApJ, 506, 686
Wahde, M., Donner, K. J., & Sandelius, B. 1996, MNRAS, 281, 1165
Weinberg, M. D. 1989, MNRAS, 239, 549
White, S. D. M. 1983, ApJ, 274, 53
Zaritsky, D., & White, S. D. M. 1988, MNRAS, 235, 289